



Contents lists available at ScienceDirect

Comptes Rendus Chimie

www.sciencedirect.com



Full paper/Mémoire

An epoxide ring-opening reaction by using sol–gel-synthesized palladium supported on a strontium hydroxyl fluoride catalyst

Vaibhav R. Acham^a, Mohan K. Dongare^{a, b}, Erhard Kemnitz^{c, **},
Shubhangi B. Umbarkar^{a, *, 1}

^a Catalysis and Inorganic Chemistry Division, CSIR – National Chemical Laboratory, Dr. Homi Bhabha Road, Pune, 411008, India

^b Malati Fine Chemicals Pvt. Ltd., Panchwati, Pashan Road, Pune, 411008, India

^c Humboldt University Berlin, Institute of Chemistry, Brook-Taylor-Straße 2, 12489, Berlin, Germany

ARTICLE INFO

Article history:

Received 20 July 2015

Accepted 11 July 2016

Available online xxxx

Keywords:

Heterogeneous catalysis

Strontium fluoride

Epoxides

Alcoholysis

β -Hydroxy alcohols

ABSTRACT

Palladium supported on a strontium hydroxyl fluoride catalyst was synthesized by a one-pot fluorolytic sol–gel method. The prepared catalyst was characterized by various physicochemical techniques. The sol–gel method has led to the formation of a high surface area ($57 \text{ m}^2 \text{ g}^{-1}$), mesoporous (pore diameter = 13.0 nm) catalyst with uniform dispersion of Pd nanoparticles of size $\sim 7 \text{ nm}$ on the surface of strontium hydroxyl fluoride. The catalyst was used for epoxide alcoholysis, and 100% conversion was obtained with 96% selectivity for β -alkoxy alcohols under mild conditions. The catalyst could be recycled for up to three catalytic cycles without any appreciable decrease in conversion and selectivity, indicating the stability of the catalyst under the reaction conditions. Further, the mechanism of alcoholysis was proposed on the basis of the physicochemical characteristics of the catalyst and on the basis of the products formed during the catalytic reaction.

© 2016 Académie des sciences. Published by Elsevier Masson SAS. All rights reserved.

1. Introduction

Epoxides are resourceful and vital intermediates in the organic synthesis which, undergoes ring-opening reactions to give β -substituted compounds with a variety of nucleophilic species [1]. Epoxides undergo a variety of ring-opening reactions to give β -amino alcohols [2], 1,2-diacetates [3], carbonyl compounds [4], diols [5], β -alkoxy alcohols [6], and β -alkoxy sulfides [7]. This is the convenient, practical and widely employed strategy for the

synthesis of important classes of intermediates in organic chemistry. The opening of epoxides with alcohols is one of the important transformations for the synthesis of β -alkoxy alcohols which are mainly used as valuable organic solvents, versatile synthons, and intermediates [8].

A variety of organic reactions that are catalyzed by Brønsted acids such as H_2SO_4 , HCl , HNO_3 , CH_3COOH , etc. or Lewis acids like AlCl_3 , TiCl_4 , FeCl_3 , ZnCl_2 , etc. has been gradually replaced by heterogeneous catalysts with more efficiency [9]. The conventional mineral acids or bases have been used for alcoholysis of epoxides, which resulted in the formation of polymerized products with low regioselectivity [10]. The use of conventional mineral acids in industrial processes is still widespread, leading to large amounts of inorganic waste, often imposing drastic reaction conditions.

Various catalysts have been used for this transformation including Lewis acids such as FeCl_3 [11], $\text{Cu}(\text{BF}_4)_2 \cdot n\text{H}_2\text{O}$

This article is dedicated to Prof. Edmond Payen on his 60th birthday.

* Corresponding author.

** Corresponding author.

E-mail addresses: vaibhav.acham@gmail.com (V.R. Acham), dongare.mohan@gmail.com (M.K. Dongare), erhard.kemnitz@chemie.hu-berlin.de (E. Kemnitz), sb.umbarkar@ncl.res.in (S.B. Umbarkar).

¹ URL http://academic.ncl.res.in/ncl_1/sb.umbarkar.

<http://dx.doi.org/10.1016/j.crci.2016.07.008>

1631-0748/© 2016 Académie des sciences. Published by Elsevier Masson SAS. All rights reserved.

Please cite this article in press as: V.R. Acham, et al., An epoxide ring-opening reaction by using sol–gel-synthesized palladium supported on a strontium hydroxyl fluoride catalyst, Comptes Rendus Chimie (2016), <http://dx.doi.org/10.1016/j.crci.2016.07.008>

[12], InCl_3 [13], $\text{Mg}(\text{HSO}_4)_2$ [14] and heterogeneous catalysts like polymer supported FeCl_3 [15] and $\text{AlPW}_{12}\text{O}_{40}$ [16]. Recently, the use of triflates $\text{Yb}(\text{OTf})_3$ [17] and perchlorates $\text{Fe}(\text{ClO}_4)_3$ [18] has been reported along with other catalysts such as Cp_2ZrCl_2 [19], $\text{K}_5[\text{CoW}_{12}\text{O}_{40}] \cdot 3\text{H}_2\text{O}$ [20], CBr_4 [21], tin(IV) porphyrinato trifluoromethanesulfonate [22], and Amberlyst-15 [23] for the alcoholysis of epoxides. Although currently there are a number of methods available for epoxide ring opening, they have one or more disadvantages, such as a long reaction time, high catalyst loading, high reaction temperature, tedious method of catalyst synthesis, and low selectivity. However, in spite of high catalytic activity, perchlorates and triflates are less favored because of their explosive nature and high cost.

The use of harsh reaction conditions is necessary owing to poor nucleophilicity of alcohols, which led to the decrease in regioselectivity of the product [24]. Furthermore, significant and important progress has been made in the development of efficient catalytic methods which are successful under mild conditions [12,25].

The novel nanoscopic partially hydroxylated inorganic fluoride materials with bi-acidic (Lewis/Brønsted) properties were developed for catalytic applications [26]. The materials were synthesized using classical sol–gel route from metal alkoxide via fluorination with aqueous/non-aqueous HF which led to high surface area metal fluorides [27]. These types of catalysts have been already applied successfully for various catalytic applications viz. synthesis of (all-rac)- $[\alpha]$ -tocopherol [28], Friedel–Crafts reaction [29], Suzuki coupling reaction [30], synthesis of menthol [31], synthesis of vitamin K-1 and K-2 chromanol [32], oxidation of ethylbenzene [33], dehydrohalogenation of 3-chloro-1,1,1,3-tetrafluorobutane [34], catalytic C–H bond activation [35] and glycerol acetylation [36].

Recently the palladium supported catalyst was used for phenolysis of epoxides at a high temperature in the presence of bases [37]. The Pd supported on alkaline earth metal fluoride is known for its dual (acidic/basic) properties. These properties play an important role in determining not only the activity but also the selectivity of the catalytic reactions. Therefore the study of synthesis and characterization of palladium supported strontium fluoride and its catalytic activity for alcoholysis of epoxides has been carried out and the results are presented in this article.

2. Experimental

2.1. General

All chemicals were procured from Aldrich Chemical Co., USA and used as received. Hydrofluoric acid (71% aq. solution) and solvents were procured from Merck Chemicals, Germany and used as obtained.

2.2. Catalyst synthesis

Cautions:

1. HF is a highly toxic and irritant compound causing severe burns if it comes in contact with the skin.

2. Strontium is highly reactive with methanol to generate hydrogen hence the rate of reaction needs to be controlled by keeping the reaction flask in an ice bath.

Catalyst preparation was carried out under an inert atmosphere of argon using a standard Schlenk technique. In a 250 mL round bottom flask, metallic strontium (2.103 g, 24 mmol) was treated with dry methanol (300 mL) at room temperature for 16 h in a Schlenk flask to form strontium methoxide solution. A stoichiometric amount (Sr/F: 1/2) of 71% aqueous solution of hydrofluoric acid (5.3 mL, 48 mmol) was added to the solution of strontium methoxide followed by the addition of alcoholic solution of palladium acetate (0.630 g, 1 wt % loading of Pd metal, dissolved in 15 mL of methanol). This solution turned into a gray colored gel which was kept for 16 h for aging. Then the gray gel was dried under vacuum at room temperature and 70 °C to remove solvents (methanol and water). The solid product was further calcined at 250 °C for 5 h. The prepared catalyst is referred hereafter as Pd-SrF₂-71 indicating 71% aqueous concentration of HF used for synthesis.

Similarly, other fluoride based catalysts Pd-MF₂-71 (where, M = Mg, Sr, Ba) were also prepared for comparison of catalytic activity.

2.3. Catalyst characterizations

The Pd-SrF₂-71 was characterized using various physicochemical techniques as mentioned below.

2.3.1. Powder X-ray diffraction (PXRD) analysis

Crystallinity and phase purity of the samples were determined using powder X-ray diffraction (PXRD) analysis. Powder patterns were recorded on an X'pert Pro PANalytical X-ray diffractometer with Ni-filtered Cu-K α radiation (40 kV, 30 mA) in the 2 θ range of 10–80° at a scan rate of 4 min^{−1} on the glass substrate.

2.3.2. FTIR spectroscopy

A Nicolet Nexus 670 FTIR instrument with a DTGS detector was used to record the IR spectrum of the catalyst in the range 4000–400 cm^{−1} with a KBr pallet technique in transmission mode. The data were collected at 4 cm^{−1} resolution averaged over 100 scans.

2.3.3. BET surface area measurements

The specific surface area (BET) of the sample was determined by acquiring adsorption–desorption isotherm (BET method) at 77 K for nitrogen gas using a Autosorb Quanta Chrome corporation instrument. The micropore volume was estimated from the t-plot and the pore diameter was estimated using the Barrett–Joyner–Halenda (BJH) model.

2.3.4. Ammonia-temperature programmed desorption (NH₃-TPD) analysis

NH₃-TPD measurements were performed on a Micromeritics AutoChem 2910 instrument. In a typical experiment, 0.1 g of the catalyst was taken in a U-shaped, flow-thru, quartz sample tube. Prior to measurements, the

catalyst was pre-treated in helium ($30 \text{ cm}^3 \text{ min}^{-1}$) at 250°C for 1 h. A mixture of NH_3 in helium (10%) was passed ($30 \text{ cm}^3 \text{ min}^{-1}$) at 25°C for 1 h. The sample was subsequently flushed with helium ($30 \text{ cm}^3 \text{ min}^{-1}$) at 100°C for 1 h. The TPD measurements were carried out in the range $100\text{--}250^\circ\text{C}$ at a heating rate of $10^\circ\text{C min}^{-1}$. The ammonia concentration in the effluent was monitored with a gold-plated, filament thermal conductivity detector (TCD). The amount of desorbed ammonia was determined based on the area under the peak.

2.3.5. X-ray photoelectron spectroscopy (XPS)

XPS was recorded using a VG Micro Tech ESCA 3000 instrument at a pressure below 10^{-9} Torr. The samples were mounted on sample tubes. The wide scan C-1s, O-1s, F-1s, Pd-3d and Mg-2p core level spectra were recorded with monochromatic Al K α radiation (photon energy = 1486.6 eV) at the pass energy of 50 eV and electron take-off angle of 60° . The core-level binding energies were aligned taking 'adventitious' carbon's binding energy as 284.6 eV . All peaks were fitted with Gauss–Lorentz peaks using XPSPEAK41 software to obtain peak information. A Shirley's baseline was used in the fitting process.

2.3.6. Scanning electron microscopy (SEM)

The elemental composition on the catalyst surface and catalyst morphology was determined by EDAX analysis coupled with FEI Quanta, 200 3D SEM using an aluminum sample holder on the carbon film.

2.3.7. Transmission electron microscopy (TEM)

The palladium particle size was determined using HRTEM measurements on a Tecnai F 30 instrument operated at an accelerating voltage of 200 kV . The TEM grids were prepared by dispersing the powder in 2-propanol using ultrasound. The suspension was dropped by the micropipette on a conventional carbon film with a thickness of about 20 nm supported by a copper grid. After complete evaporation of the 2-propanol from the specimen, the TEM imaging was performed.

2.4. Typical procedure for the catalytic reaction

In a sample tube equipped with a magnetic needle, an epoxide (1.0 mmol), alcohol (2.0 mL) and catalyst (10 wt % with respect to epoxide) were added. The reaction mixture was stirred at room temperature for the given time. The progress of the reaction was monitored by thin layer chromatography (TLC) and gas chromatography (GC). After the completion of the reaction, the catalyst was separated by filtration and washed with alcohol and diethyl ether. The combined organic fractions were dried over anhydrous sodium sulfate and the solvent was removed under reduced pressure. The reaction was monitored by gas chromatographic analysis using an Agilent 6890 Gas Chromatograph equipped with a HP-5 dimethyl polysiloxane capillary column (60 m length, 0.25 mm internal diameter, $0.25 \mu\text{m}$ film thickness) with a flame ionization detector. Products were confirmed by comparison with GC spectra of the authentic samples. Further, the structure was confirmed by FTIR (Nicolet Nexus spectrometer equipped

with a DTGS detector) and ^1H NMR (Bruker AC 200, 200 MHz spectrometer) spectral analysis and matched with the literature (only for representative reaction alcoholysis of cyclohexene oxide, styrene oxide and epichlorohydrin using ethanol).

2.5. Procedure for the catalytic recycle study

To study the recyclability of the catalyst, after completion of the first reaction, the catalyst was separated using centrifugation followed by filtration through Whatman filter paper no. 1, washed with ethanol ($5 \text{ mL} \times 3$ times), and finally dried at 80°C for 30 min. A fresh charge of reactants was taken with the dried catalyst and subjected to similar reaction conditions. The same procedure was repeated for successive three catalytic runs with the same catalyst.

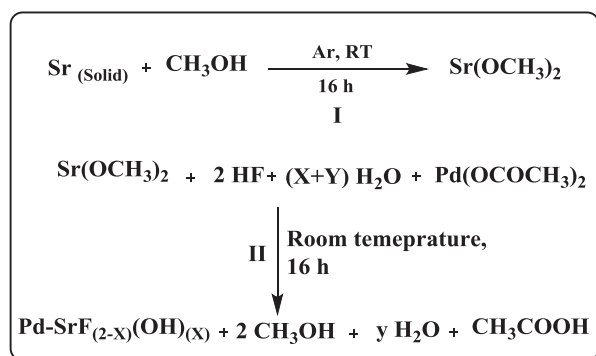
2.6. Procedure for the filtration experiment study and ICP analysis

To verify the Pd leaching in the reaction mixture, the filtration test was carried out at room temperature. A 0.05 g of the catalyst was stirred with 0.5 g of cyclohexene oxide in 6 mL of ethanol under typical reaction conditions at room temperature. After 1 h, the catalyst was separated from the liquid phase by centrifugation followed by filtration through Whatman filter paper No. 1. Further, the reaction was continued without the catalyst at room temperature. The separated catalyst was further tested for ICP-AES analysis to determine the Pd content in the catalyst. The catalyst sample was mixed with a solution of conc. HNO_3 (20% v/v) in a 50 mL PFA beaker (ratio of acid solution to sample = ~ 50 by weight). The sample was heated in the bomb at 100°C in the oven for 3 h. After cooling the sample, the solution was taken out in a volumetric flask. The solution was then diluted to 100 mL using milli Q water by using a calibrated volumetric flask, which was further subjected to ICP analysis. Metal leaching was studied by ICP-AES analysis of the catalyst before and after the three reaction cycles.

3. Results and discussion

3.1. Catalyst synthesis

The one pot synthesis of the Pd-SrF $_2$ -71 catalyst by the fluorolytic sol–gel route using aq. HF (71%), resulted in simultaneous fluorolysis and hydrolysis of M–OR bond to form M–F and M–OH bonds, respectively [38,39]. Though the molar ratio of Sr:HF was adjusted to 1:2, the hydrolysis of strontium methoxide becomes competitive with the fluorination due to water content in the fluorinating agent. This reaction generates the composition in which both fluorine and hydroxide are attached to strontium in a solid structure and this led to the formation of strontium hydroxyl fluorides $[\text{SrF}_{(2-x)}(\text{OH})_x]$ material, which upon further addition of methanolic solution of palladium acetate forms Pd-SrF $_{2-x}(\text{OH})_x$ (henceforth referred to as Pd-SrF $_2$ -71) catalyst as represented in Scheme 1. The addition of an alcoholic solution of palladium acetate led to the



Scheme 1. Schematic representation for sol–gel synthesis of the Pd-SrF₂-71 catalyst.

formation of light red colored gel initially which upon aging turned light gray. Typically Pd^{II} gets partially reduced to Pd⁰ due to dissolved hydrogen liberated during the formation of strontium methoxide from metallic strontium to give gray color to the gel. In contrast to the non-aqueous sol–gel route which results in the formation of clear sols and transparent gels, the aqueous route results in opaque gels of gray color due to the presence of partially reduced palladium nanoparticles [40]. The bulk and surface structure of this material was characterized using various physicochemical techniques.

3.2. XRD

The PXRD pattern of the prepared sample is shown in Fig. 1. The diffraction peaks can be indexed as the peak corresponding to metal fluorides and metal hydroxides on comparison with strontium fluoride (JCPDS 06-0262) and strontium hydroxide (JCPDS 27-847). Furthermore, PXRD showed broad peaks which may correspond to strontium fluoride and sharp peaks to strontium hydroxide. Additionally, few less intense peaks were observed; these peaks indicate the formation of mixed phases of strontium

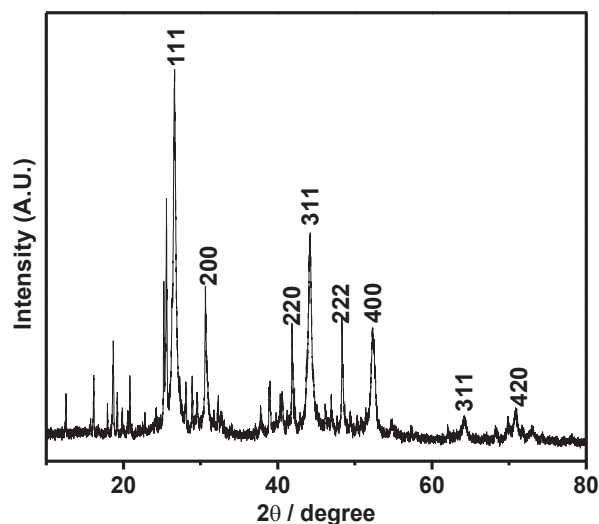


Fig. 1. PXRD pattern of the Pd-SrF₂-71 catalyst.

hydroxyl fluorides. However, no diffraction for Pd₁₁₁ was detected because of a very low content of Pd with high order of dispersion of Pd particles over the surface of the catalyst.

3.3. FTIR

The FTIR spectrum of the Pd-SrF₂-71 catalyst showed the bands at 3450, 3007, 1631, 1402, 1083, 743, and 484 cm⁻¹ (Fig. 2). The intense bands at 484 and 743 cm⁻¹ can be related to ν(Sr–F) and ν(Sr–O), respectively. The bands around 3450 and 1650 cm⁻¹ correspond to the presence of surface hydroxyl groups or moisture. The band at 3007 and 1083 cm⁻¹ observed due to ν(C–H) and ν(C–O) stretching vibrations could be due to the hydrocarbon residue in prepared catalysts. The presence of Sr–O and O–H band confirms the formation of the partially hydroxylated strontium fluoride phase in the final catalyst [41].

3.4. BET surface area

Nitrogen sorption studies were performed to study the surface area, pore diameter and pore volume (Fig. 3). The isotherms showed type IV character typical for mesoporous materials with a H1 type hysteresis loop and porous texture. The BET surface area and total pore volume of the catalyst was found to be 57 m²g⁻¹ and 0.11 cc g⁻¹, respectively. Typically the surface area of Pd-SrF₂-71 was observed to be intermediate between metal fluorides from the same group in the periodic table like Pd-MgF₂-71 (140 m²g⁻¹) and Pd-BaF₂-71 (8 m²g⁻¹) prepared under identical conditions. The average pore size was determined using Barrett–Joyner–Halenda (BJH) analysis and found to be 13.1 nm, which confirms the mesoporous nature of the catalyst.

3.5. Acidity measurements

3.5.1. Ammonia-temperature programmed desorption (NH₃-TPD)

The total acidity as well as the strength of acidic sites on the surface of the catalysts was determined by ammonia-

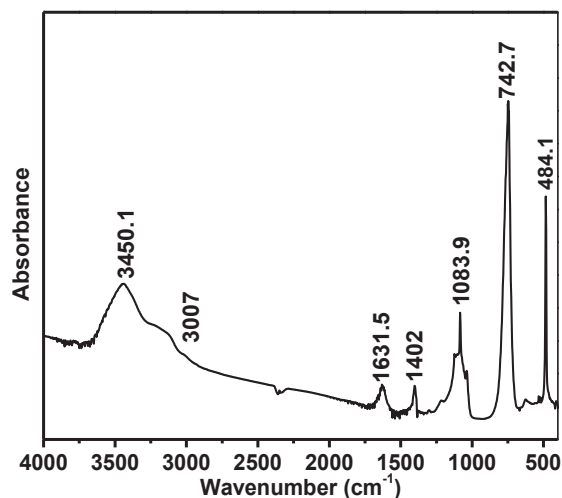


Fig. 2. FTIR spectrum of the Pd-SrF₂-71 catalyst.

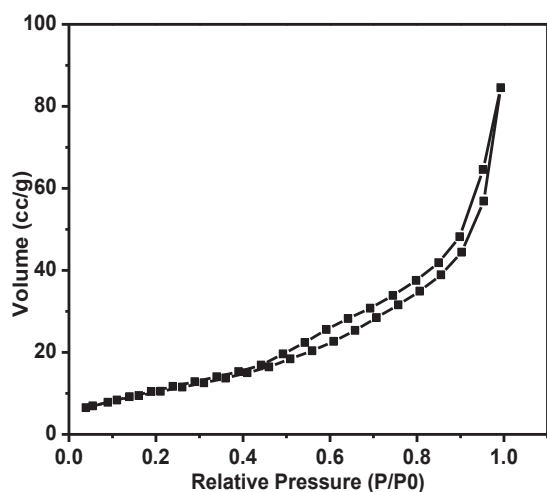


Fig. 3. BET surface area plot of the Pd-SrF₂-71 catalyst.

temperature programmed desorption (NH₃-TPD) technique as shown in Fig. 4. The NH₃ desorption studies indicated the presence of weak, moderate and strong acidic sites with peak maxima corresponding to 111, 276, and 386 °C, respectively. Also, the total acidity of the catalyst was found to be 0.151 mmol g⁻¹. The total acidity of the catalyst was dependant on the degree of fluorination as well as on the nature of the metal alkoxide. Normally a decreasing trend in the acidity of the metal alkoxide was observed down the group in the periodic table.

3.5.2. FTIR of adsorbed pyridine

The type of acidity present on the catalyst surface was studied by DRIFT spectroscopy of adsorbed pyridine ($pK_a = 5.25$). The subtracted FTIR spectrum of adsorbed pyridine on the Pd-SrF₂-71 surface is shown in Fig. 5. The FTIR peak at 1445 and 1545 cm⁻¹ shows the presence of Lewis and Brønsted acidic sites, respectively, while the peak at 1490 cm⁻¹ represents the presence of both Lewis

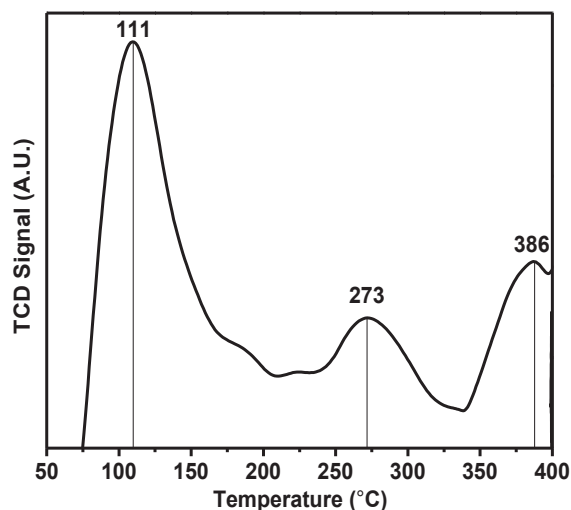


Fig. 4. NH₃-temperature program desorption plot of the Pd-SrF₂-71 catalyst.

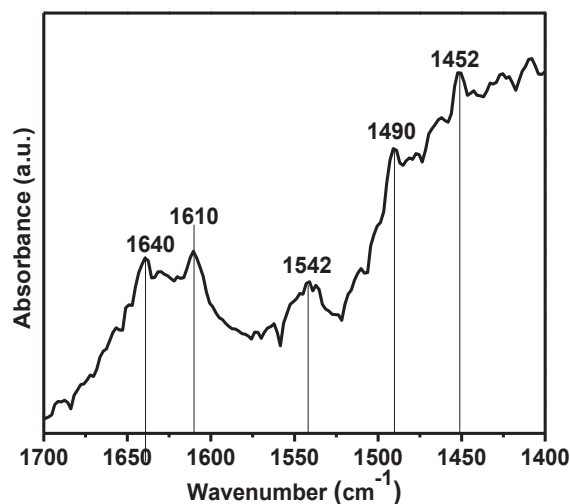


Fig. 5. FTIR spectrum of adsorbed pyridine on the Pd-SrF₂-71 surface at 100 °C.

and Brønsted acidity on the surface of oxide materials in adsorbed pyridine spectrum [42]. Similarly, the bands in the adsorbed pyridine spectrum of Pd-SrF₂-71 are assignable to coordinately bound pyridine [42,43]. The pyridinium ion (PyH⁺) produced by the reaction of pyridine with Brønsted acid sites showed bands around 1542 and 1640 cm⁻¹. The coordinately bound pyridine on Lewis acid sites shows bands around 1452 and 1610 cm⁻¹. This DRIFT indicated the presence of Lewis and Brønsted acidic sites on the surface of the Pd-SrF₂-71 catalyst.

3.6. XPS

XPS was used to derive surface compositional information of the Pd-SrF₂-71 catalyst in Fig. 6. The montage of the survey scan after analysis of the Pd-SrF₂-71 catalyst is shown in Fig. 6-A. The peaks were annotated to the Sr, F, O and Pd with their core levels. The peaks were standardized with respect to the carbon peak at 284.6 eV on the surface. Due to non-conductive nature of strontium fluoride, some charging of the sample was observed. In order to determine the effect of the support on the oxidation state of palladium of the as-synthesized samples, the region of Pd was studied further (Fig. 6-B). Palladium showed the presence of two oxidation states namely Pd⁰ and Pd²⁺. The two different values of Pd²⁺ may be due to variable coordination of Pd²⁺ species. The peak at 335.1 corresponds to Pd⁰ and peaks at 338.9 and 340.4 relate to Pd²⁺ species from palladium acetate and palladium oxide, respectively [44]. The ratio of relative abundance (Pd: Pd²⁺) was observed to be 1:2 approximately. The presence of Pd⁰ can be attributed to the partial reduction of palladium acetate in the presence of dissolved hydrogen which was produced during catalyst synthesis.

3.7. SEM

The morphology of the Pd-SrF₂-71 catalyst was studied by SEM. The representative micrograph of Pd-SrF₂-71 is

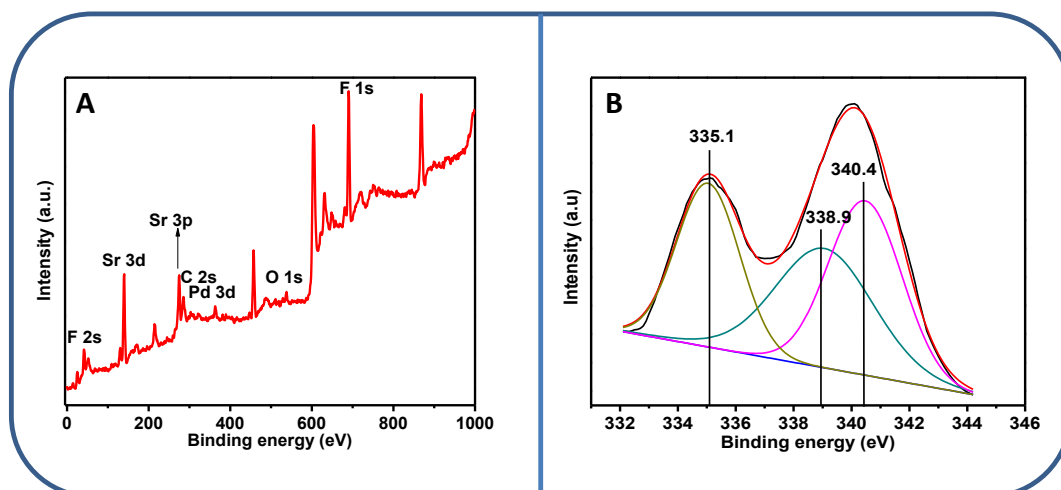


Fig. 6. XPS of the Pd-SrF₂-71 catalysts; (A) survey scan and (B) scan for binding energy of palladium species.

shown in Fig. 7-a. It showed the particles of SrF₂-71 to be oval-shaped of 1.5–2.0 μm in length and 0.5–1.0 μm in width. The Pd particles were spread throughout evenly on the strontium hydroxyl fluoride surface. Further, the surface composition of the catalyst was also determined by EDAX spectroscopy. The results showed the surface palladium composition to be approximately 1.1 wt %.

3.8. TEM

The particle size of palladium was determined by HRTEM analysis. The representative micrograph of Pd-SrF₂-71 is shown in Fig. 7-b. The particle size distribution studied by TEM clearly showed the majority of particles with ~ 7 nm diameter though the particle size distribution spreads over a wide range. There is clearly the bimodal distribution of Pd particles observed in TEM. Many particles

are in the range of 7–10 nm where as many Pd particles are of large sizes of around 20–30 nm. Some agglomerated Pd was also observed in TEM. The palladium particles were found to be in 111 planes as identified from d spacing ($d_{111} = 0.223$ nm).

3.9. Catalytic activity for alcoholysis of epoxides

The catalytic activity of Pd-MF₂-71 (where, M = Mg, Sr, Ba) was studied for alcoholysis of epoxide at room temperature initially with cyclohexene oxide as the model substrate and ethanol as nucleophile (Scheme 2). The results obtained with various catalysts are given in Table 1. In the absence of the catalyst, the reaction did not take place even after 2 h time (Table 1, entry 1). Further a series of palladium supported metal fluoride catalysts were evaluated for catalytic reactions. The Pd-MgF₂-71, Pd-SrF₂-71,

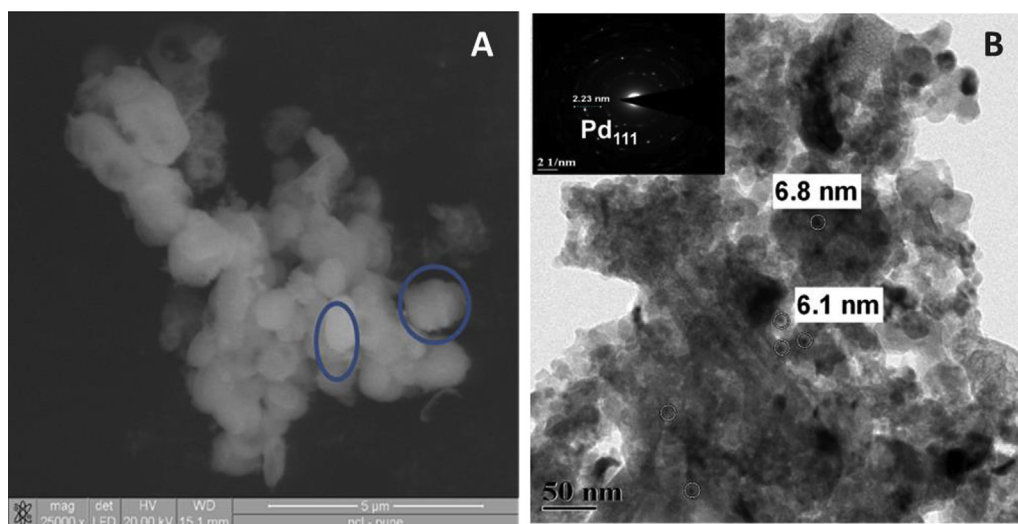


Fig. 7. Representative electron microscopic image of the Pd-SrF₂-71 catalyst (A) SEM image and (B) TEM image SAED pattern.

and Pd-BaF₂-71 catalysts showed 43, 100 and 20% conversion, respectively (Table 1, entry 2–4). It is well known that the Lewis acidity of the catalyst decreases from Pd-AlF₃ to Pd-BaF₂ with the increase in basicity [45]. In the case of a highly acidic catalyst, higher conversion has been reported but the higher order of acidity is responsible for the decrease in selectivity and generation of byproduct like 1,6-hexandiol. Moreover, Pd-BaF₂ showed less conversion with 100% selectivity due to its basic nature. In the case of Pd-SrF₂, the acidic and basic sites were found to be balanced to get optimum conversion and selectivity. The catalytic activity of the Pd-AlF₃ was compared which showed 59% conversion under identical reaction conditions (Table 1, entry 5).

3.10. Effects of various reaction parameters

3.10.1. Catalyst loading effect

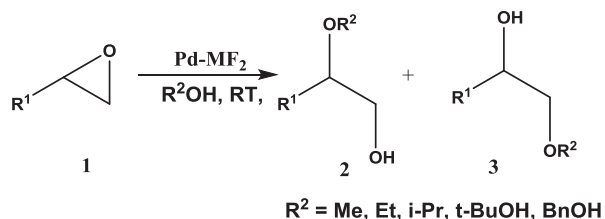
The effect of catalyst loading on alcoholysis of cyclohexene oxide was studied at room temperature in Fig. 8. The conversion increased with gradual increase in catalyst loading. The 1 wt % catalyst loading gave 9% conversion which increased to 70% for 15 wt % loading in 1 h at room temperature. There was a marginal decrease in selectivity at high catalyst loading.

3.10.2. Temperature effect

Epoxide ring opening of cyclohexene oxide was studied at various temperatures ranging from room temperature to 70 °C in ethanol with 10 wt % loading of the Pd-SrF₂-71 catalyst as shown in Fig. 9. It was observed that with the gradual increase in the reaction temperature from room temperature (27 °C) to 70 °C, the time for 100% conversion of cyclohexene oxide decreased from 120 to 30 min without much decrease in selectivity. The increase in the rate of reaction can be correlated to increase in the rate of intermolecular collision. Although the rate of reaction was higher at 70 °C, room temperature is always preferred. Therefore room temperature was considered as the optimum temperature for carrying out further reactions.

3.10.3. Time profile study

The conversion of the cyclohexene oxide increased with increase in the reaction time at room temperature in ethanol as shown (Fig. 10). A virtually linear time-conversion profile has been observed for ethanolysis of cyclohexene oxide. The selectivity of the 2-ethoxycyclohexanol decreased to 96% after complete conversion of cyclohexene oxide after 2 h which was found to be constant up to 2.5 h at room temperature.



Scheme 2. Alcoholysis of epoxides.

Table 1
Results of alcoholysis of epoxide.^a

Entry	Catalyst	Conv. ^b (%)	Sel. ^b (%)	Activity ^c (mmol h ⁻¹ g ⁻¹) × 10 ⁴
1	None	0	—	—
2	Pd-MgF ₂ -71	43	93	3.18
3	Pd-SrF ₂ -71	100	96	7.00
4	Pd-BaF ₂ -71	20	96	1.27
5	Pd-AlF ₃ -71	59	80	2.86

^a Reaction conditions: Cyclohexene oxide: 1 mmol; ethanol: 2 mL; catalyst: 0.01 g (1.0 wt % of Pd loading); temperature: RT (27 °C), time: 2 h.

^b Conv. and Sel. were determined based on GC results.

^c Rate constants were determined by assuming the reaction to follow first-order kinetics for 30 min of time.

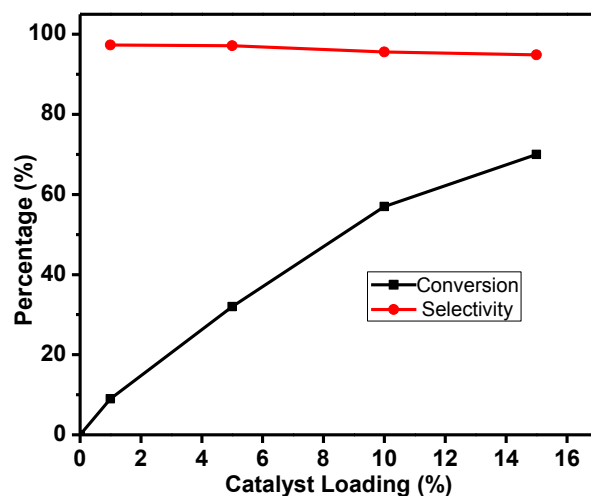


Fig. 8. Catalyst loading effect using the Pd-SrF₂-71 catalyst. Reaction conditions: cyclohexene oxide: 5 mmol (0.54 g); ethanol: 2 mL; temperature: RT (27 °C). Time: 1 h.

3.11. Substrate scope study

After optimizing the reaction conditions for ethanol as a nucleophile with cyclohexene oxide as a model reaction,

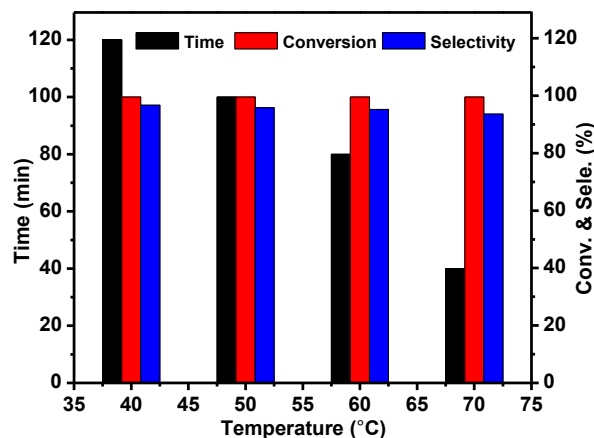
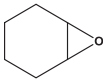
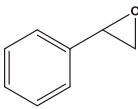
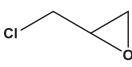


Fig. 9. Temperature effect study using the Pd-SrF₂-71 catalyst. Reaction conditions: cyclohexene oxide: 2 mmol (0.196 g); catalyst (Pd-SrF₂): 0.02 g; ethanol: 2 mL.

the applicability of the catalyst to other epoxides and alcohols was evaluated. The reaction of cyclohexene oxide with methanol and ethanol gave 98 and 96% yields, respectively (Table 2, entry 1–2). The reaction of 2-propanol gave a lower yield (57%) as compared to ethanol as a nucleophilic source (Table 2, entry 3). This may be due to the steric effect of two methyl groups, which hinders the reaction site resulting in the lowering of cyclohexene oxide conversion into the desired product. A similar behavior was observed when the reaction was carried out with *t*-butyl alcohol, which showed a 25% yield (Table 2, entry 4). This observation can be explained by the fact that *tertiary* butyl alcohol is even more bulky, having three methyl groups which increases the steric hindrance and lower the activity in the nucleophilic substitution reaction. When benzyl alcohol was used as the nucleophile, a 99% yield was observed (Table 2, entry 5). Although the steric hindrance in benzyl alcohols is higher than that in *t*-butyl alcohol, the higher nucleophilicity may be responsible for increment in the rate of the reaction. Further, styrene oxide was used as the substrate to check the effect of the catalyst on regio-selectivity (Table 2, entry 5–10).

The rate of the reaction was found to be dependant on nucleophilicity of the alcohol but also on the steric hindrance of epoxide. The yields of β -alkoxy alcohols decreased from methoxy to *t*-butoxy (92–18%) due to increasing bulkier nature of nucleophile (Table 2, entry 5–9), which increased to 72% in the case of benzyl alcohol (Table 2, entry 10). The reaction of epichlorohydrin with methanol and ethanol showed 89 and 78% yields, respectively (Table 2, entry 11–12). When bulkier alcohols like 2-propanol and 2-methyl-2-propanol were used as the nucleophile, the yield decreased to 53 and 36%, respectively (Table 2, entry 13–14), which again increased to 65% with benzyl alcohol as the nucleophile (Table 2, entry 15). Remarkably, the formation of a single regioisomer was observed in all the cases. This formation of a stable intermediate in each case led to the formation of a single regioisomer. In styrene, because of formation of stable

Table 2Substrate scope study using the Pd-SrF₂-71 catalyst.^a

Entry	Epoxide	Alcohol	Products ratio (2:3)	Yields ^b (%)
1		MeOH	<i>Trans</i>	98
2		EtOH	<i>Trans</i>	96
3		<i>i</i> -PrOH	<i>Trans</i>	57
4		<i>t</i> -BuOH	<i>Trans</i>	25
5		BnOH	<i>Trans</i>	99
6		MeOH	100:0	92
7		EtOH	100:0	73
8		<i>i</i> -PrOH	100:0	49
9		<i>t</i> -BuOH	100:0	18
10		BnOH	100:0	72
11		MeOH	0:100	89
12		EtOH	0:100	78
13		<i>i</i> -PrOH	0:100	53
14		<i>t</i> -BuOH	0:100	36
15		BnOH	0:100	65

^a Reaction conditions: substrate: 0.2 g; catalyst (Pd-SrF₂-71): 0.02 g (10 wt % w.r.t. substrate); alcohols: 2 mL; temperature: RT (27 °C). Time: 2 h.

^b Yields were determined based on GC.

benzylic carbocation, the reaction follows the S_N¹ pathway and formed **2** as the preferable regio-isomer. In epichlorohydrin, the reaction follows the S_N² pathway due to the attack of the nucleophile from the rear side of the ring opening, yielding **3** as the preferable regioisomer.

3.12. Catalyst recycle study

The recyclability of Pd-SrF₂-71 was studied for the ring opening of cyclohexene oxide in ethanol under optimized reaction conditions. After completion of the reaction, the catalyst was separated from the reaction mixture by centrifugation followed by filtration using Whatman filter paper no.1. The catalyst was washed with ethanol (5 mL \times 2) and acetone (5 mL) and allowed to dry at 80 °C and used it for subsequent catalytic runs. The same procedure was repeated for three times. However, even after three runs, the catalyst exhibited excellent activity as shown in Fig. 11. It implied that the catalytic system can be

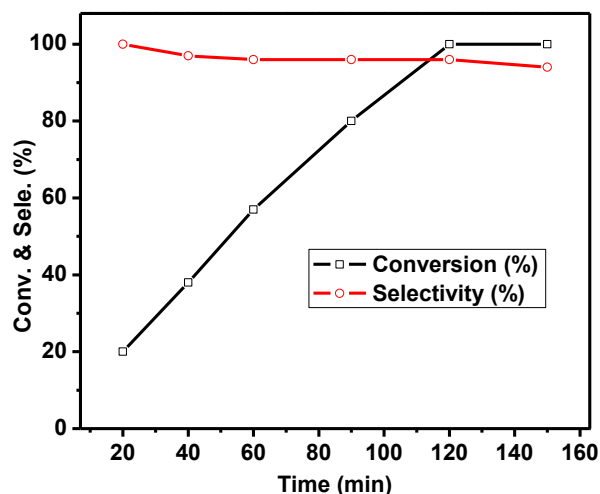


Fig. 10. Time profile study using the Pd-SrF₂-71 catalyst. Reaction conditions: cyclohexene oxide: 2 mmol (0.196 g); catalyst (Pd-SrF₂-71): 0.02 g (10 wt % of cyclohexene oxide); ethanol: 2 mL; temperature: RT (27 °C).

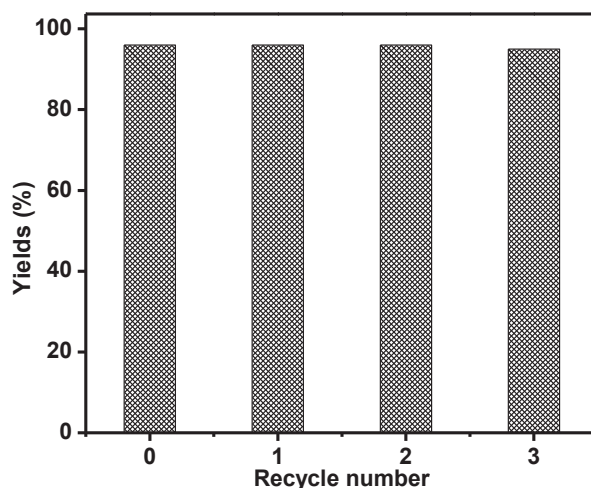


Fig. 11. Recycle study using the Pd-SrF₂-71 catalyst. Reaction conditions: cyclohexene oxide: 5 mmol (0.54 g); Pd-SrF₂-71: 0.05 g (10 wt % w.r.t. substrate); ethanol: 2 mL; temperature: RT (27 °C). Time: 2 h.

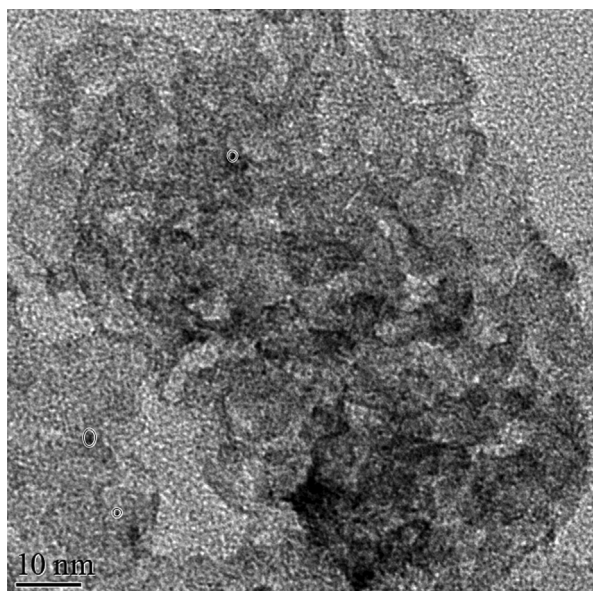


Fig. 12. TEM image of the Pd-SrF₂-71 catalyst after third catalytic recycle.

used even for three cycles without significant loss of activity.

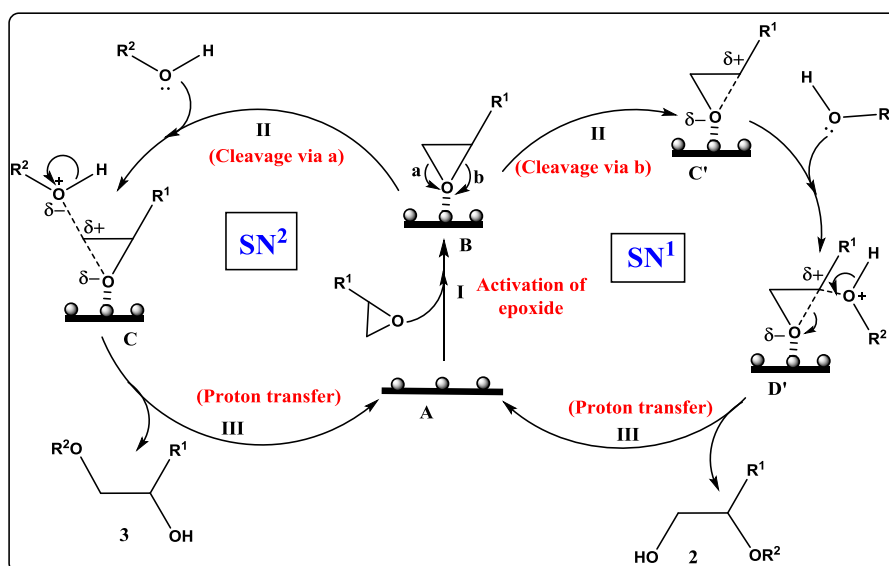
3.13. TEM and ICP analysis of recycled catalyst

The TEM image of the recycled catalyst after third cycle revealed no agglomeration of Pd on the catalyst surface as shown in Fig. 12. The size of the Pd nanoparticle was found to be in the same range of 6–8 nm when compared with that of the fresh catalyst (refer Fig. 7). There was no decrease in the catalytic activity in successive cycles for alcoholysis of epoxides. The filtration test was used to check the Pd leaching in the reaction mixture. It was observed that in the absence of the catalyst, no further

change in cyclohexene oxide conversion was observed even after additional 3 h which confirms no Pd leaching which was also confirmed by ICP-AES analysis of the catalyst. The Pd concentration was found to be 0.986% before the reaction and 0.978% after the reaction. Therefore the Pd-SrF₂-71 catalyst acts as a true heterogeneous catalytic system.

3.14. Possible reaction mechanism

Based on the results obtained during catalytic reactions and by comparison with the literature reports, the mechanism for the alcoholysis of epoxide using the Pd-SrF₂-71 catalyst has been proposed in Scheme 3. In the case of styrene oxide, the nucleophilic alkoxy group attacks in such a way to produce 2-phenyl-2-alkoxy ethanol. While in the epichlorohydrin case, the alkoxy group attacks epoxide ring to get 3-chloro-1-alkoxy-2-propanol as the only product. Initially, the adsorption of epoxide on the surface of the catalyst takes place which activates epoxide via partial transfer of electrons of oxygen to the empty orbital of oxidized palladium to get intermediate B (Step 1). Further attack of nucleophilic oxygen led to opening of the epoxide ring in two possible ways depending on the nature of the alkyl group. In the case of an electron withdrawing alkyl group, the reaction follows the S_N2 pathway to generate intermediate carbon which undergoes simultaneous C–O bond cleavage and rear side attack of nucleophilic O-atom of alcohol followed by proton transfer to produce product 3. In the case of an electron donating alkyl group, the reaction follows the S_N1 pathway to generate intermediate carbocation C' by cleavage of C–O bond. This C' carbocation intermediate gets stabilized by resonance and inductive effects, which undergoes nucleophilic attack by the nucleophilic O-atom of alcohol followed by proton transfer to generate product 2. The high regioselectivity is due to stabilization of intermediate species on the catalyst surface and results in two different nucleophilic substitution reactions.



Scheme 3. Possible reaction mechanism for regioselective alcoholysis of epoxide using the Pd-SrF₂-71 catalyst.

4. Conclusions

In conclusion, Pd-SrF₂-71 proved to be a novel and efficient catalyst for room temperature alcoholysis of epoxides. Due to the low acidic nature of the catalyst, it may find application for the ring opening of epoxides containing acid-sensitive functional groups. The catalyst showed very high regioselectivity which depends on the nature of the alkyl group of the substrate. The one-pot method of synthesis, ease of the procedure, the high order of recyclability, regioselectivity, and mild reaction conditions showed a new synthetic application of the heterogeneous metal fluoride supported palladium catalyst in synthetic chemistry.

Acknowledgements

We thank Council of Scientific and Industrial Research (CSIR), India and Federal Ministry of Education and Research (BMBF), Germany for financial support for the collaborative project. VRA acknowledges University Grant Commission (UGC) for the research fellowship.

References

- [1] (a) T.N. Birkinshaw, In *Comprehensive Organic Functional Group Transformations*, Oxford, 1995; (b) B. Sreedhar, P. Radhika, B. Neelima, N. Hebalkar, *J. Mol. Catal. A Chem.* 272 (2007) 159; (c) B. Das, V.S. Reddy, M. Krishnaiah, Y.K. Rao, *J. Mol. Catal. A Chem.* 270 (2007) 89.
- [2] G. Bartoli, M. Bosco, A. Carlone, M. Locatelli, P. Melchiorre, L. Sambri, *Org. Lett.* 6 (2004) 3973.
- [3] G. Fogassy, C. Pinel, G. Gelbard, *Catal. Commun.* 10 (2009) 557.
- [4] D.P. Serrano, R. van Grieken, J.A. Melero, A. Garcia, *Appl. Catal. A* 319 (2007) 171.
- [5] P. Salehi, M. Dabiri, M.A. Zolfigol, M.A.B. Fard, *Phosphorus Sulfur Silicon Relat. Elem.* 179 (2004) 1113.
- [6] A.J.L. Leitao, J.A.R. Salvador, R.M.A. Pinto, M.L. Sae Melo, *Tetrahedron Lett.* 49 (2008) 1694.
- [7] J. Wu, H.G. Xia, *Green Chem.* 7 (2005) 708.
- [8] (a) T. Kino, H. Hatanaka, M. Hashimoto, M. Nishiyama, T. Goto, M. Okuhara, M. Kohsaka, H. Aoki, H. Imanaka, *J. Antibiot.* 40 (1987) 1249; (b) O. Henze, W.J. Feast, F. Gardebien, P. Jonkheijm, R. Lazzaroni, P. Leclère, E.W. Meijer, A.P.H.J. Schenning, *J. Am. Chem. Soc.* 128 (2006) 5923; (c) J.E. Arrowsmith, S.F. Campbell, P.E. Cross, J.K. Stubbs, R.A. Burges, D.G. Gardiner, K.J. Blackburn, *J. Med. Chem.* 29 (1986) 1696.
- [9] (a) J.M. Thomas, R. Raja, *Annu. Rev. Mater. Res.* 35 (2005) 315; (b) P. Botella, A. Corma, S. Iborra, R. Montón, I. Rodríguez, V. Costa, *J. Catal.* 250 (2007) 161.
- [10] W. Reeve, I. Christoffel, *J. Am. Chem. Soc.* 72 (1950) 1480.
- [11] N. Iranpoor, P. Salehi, *Synthesis* (1994) 1152.
- [12] J. Barluenga, H. Vázquez-Villa, A. Ballesteros, J.M. González, *Org. Lett.* 4 (2002) 2817.
- [13] B.H. Kim, F. Piao, E.J. Lee, J.S. Kim, Y.M. Jun, B.M. Lee, *Bull. Korean Chem. Soc.* 25 (2004) 881.
- [14] P. Salehi, M.M. Khodaei, M.A. Zolfigol, A. Keyvan, *Synth. Commun.* 33 (2003) 3041.
- [15] R.V. Yarapathi, S.M. Reddy, S. Tammishetti, *React. Funct. Polym.* 64 (2005) 157.
- [16] H. Firouzabadi, N. Iranpoor, A.A. Jafari, S. Malarem, *J. Mol. Catal. A Chem.* 250 (2006) 237.
- [17] (a) P.R. Likhari, M.P. Kumar, A.K. Bandyopadhyay, *Synlett* (2001) 836; (b) N. Iranpoor, B. Zeynizadeh, *Synth. Commun.* 29 (1999) 1017; (c) D.B.G. Williams, M. Lawton, *Org. Biomol. Chem.* 3 (2005) 3269.
- [18] P. Salehi, B. Seddighi, M. Irandoost, F.K. Behbahani, *Synth. Commun.* 30 (2000) 2967.
- [19] M.L. Kantam, K. Aziz, K. Jeyalakshmi, P.R. Likhari, *Catal. Lett.* 80 (2003) 95.
- [20] S. Tangestaninejad, M. Moghadam, V. Mirkhani, B. Yadollahi, S.M.R. Mirmohammadi, *Monatsh. Chem.* 137 (2006) 235.
- [21] J.S. Yadav, B.V.S. Reddy, K. Harikishan, C. Madan, A.V. Narsaiah, *Synthesis* (2005) 2897.
- [22] M. Moghadam, S. Tangestaanejad, V. Mirkhani, R. Shaibani, *Tetrahedron* 60 (2004) 6105.
- [23] Y.H. Liu, Q.S. Liu, Z.H. Zhang, *J. Mol. Catal. A Chem.* 296 (2008) 42.
- [24] (a) G.H. Posner, D.Z. Rogers, *J. Am. Chem. Soc.* 99 (1977) 8208; (b) J. Otera, Y. Niibo, N. Tatsumi, H. Nozaki, *J. Org. Chem.* 53 (1988) 275.
- [25] (a) B.M. Choudary, Y. Sudha, *Synth. Commun.* 26 (1996) 2989; (b) S.K. Yoo, J.Y. Lee, C. Kim, S.J. Kim, Y. Kim, *Dalton Trans.* (2003) 1454; (c) D. Barreca, M.P. Copley, A.E. Graham, J.D. Holmes, M.A. Morris, R. Seraglia, T.R. Spalding, E. Tondello, *Appl. Catal. A Gen.* 304 (2006) 14; (d) M.W.C. Robinson, R. Buckle, I. Mabbett, G.M. Grant, A.E. Graham, *Tetrahedron Lett.* 48 (2007) 4723; (e) C. Torborg, D.D. Hughes, R. Buckle, M.W.C. Robinson, M.C. Bagley, A.E. Graham, *Synth. Commun.* 38 (2008) 205.
- [26] S. Wuttke, S.M. Coman, J. Kröhnert, F.C. Jentoft, E. Kemnitz, *Catal. Today* 152 (2010) 2.
- [27] S. Wuttke, S.M. Coman, G. Scholz, H. Kirmse, A. Vimont, M. Daturi, S.L.M. Schroeder, E. Kemnitz, *Chem. Eur. J.* 14 (2008) 11488.
- [28] S.M. Coman, S. Wuttke, A. Vimont, M. Daturi, E. Kemnitz, *Adv. Synth. Catal.* 350 (2008) 2517.
- [29] N. Candu, S. Wuttke, E. Kemnitz, S.M. Coman, V.I. Parvulescu, *Appl. Catal. A* 391 (2011) 169.
- [30] P.T. Patil, A. Dimitrov, J. Radnik, E. Kemnitz, *J. Mater. Chem.* 18 (2008) 1632.
- [31] A. Negoi, S. Wuttke, E. Kemnitz, D. Macovei, V.I. Parvulescu, C.M. Teodorescu, S. Coman, *Angew. Chem. Int. Ed.* 49 (2010) 3134.
- [32] S.M. Coman, V.I. Parvulescu, S. Wuttke, E. Kemnitz, *ChemCatChem* 2 (2010) 92.
- [33] I.K. Murwani, K. Scheurell, E. Kemnitz, *Catal. Commun.* 10 (2008) 227.
- [34] K. Teinz, S. Wuttke, F. Börno, J. Eicher, E. Kemnitz, *J. Catal.* 282 (2011) 175.
- [35] M.H.G. Pechtl, M. Teltewskoi, A. Dimitrov, E. Kemnitz, T. Braun, *Chem. Eur. J.* 17 (2011) 14385.
- [36] S.B. Troncea, S. Wuttke, E. Kemnitz, S.M. Coman, V.I. Parvulescu, *Appl. Catal. B Environ.* 107 (2011) 260.
- [37] K. Seth, S.R. Roy, B.V. Pipaliya, A.K. Chakraborti, *Chem. Commun.* 49 (2013) 5886.
- [38] Y. Diao, W. Walawender, C.S. Sorensen, K.J. Klabunde, T. Ricker, *Chem. Mater.* 14 (2002) 362.
- [39] K.T. Ranjit, K.J. Klabunde, *Chem. Mater.* 17 (2005) 65.
- [40] S. Wuttke, G. Scholz, S. Rudiger, E. Kemnitz, *J. Mater. Chem.* 17 (2007) 4980.
- [41] J.R. de Oliveira Lima, Y.A. Ghani, R.B. da Silva, F.M.C. Batista, R.A. Bini, L.C. Varanda, J.E. de Oliveira, *Appl. Catal. A Gen.* 445–446 (2012) 76.
- [42] (a) J. Penzien, A. Abraham, J.A. Bokhoven, A. Jentys, T.E. Muller, C. Sievers, J.A. Lercher, *J. Phys. Chem. B* 108 (2004) 4116; (b) F. Bonino, A. Damin, S. Bordiga, C. Lamberti, A. Zecchina, *Langmuir* 19 (2003) 2155; (c) M.I. Zaki, M.A. Hasan, F.A. Al-Sagheer, L. Pasupulety, *Colloids Surf. A* 190 (2001) 261.
- [43] K. Tanaka, A. Ozaki, *J. Catal.* 8 (1967) 1.
- [44] V.R. Acham, A.V. Biradar, M.K. Dongare, E. Kemnitz, S.B. Umbarkar, *ChemCatChem* 6 (2014) 3182.
- [45] M. Feist, K. Teinz, S.R. Manuel, E. Kemnitz, *E. Thermochim. Acta* 524 (2011) 170.